

# Behavior of $\text{Al}_4\text{C}_3$ Particles During Flotation and Sedimentation in Aluminum Melts



MERTOL GÖKELMA, TRYGVE STORM AARNÆS, JÜRGEN MAIER,  
MARIA F. RENKEL, KAI ERIK EKSTRØM, BERND FRIEDRICH,  
and GABRIELLA TRANELL

$\text{Al}_4\text{C}_3$  particles form during the primary production of aluminum *via* molten salt electrolysis due to the carbon solubility and direct contact between bath, metal, and carbon anodes. Additional  $\text{Al}_4\text{C}_3$  may form during melt processing through direct contact between the melt and carbonaceous materials. As a result of their small size and similar density to aluminum, removal of aluminum carbide particles can be challenging. If not removed, carbides can produce inclusion defects or poor surface condition in aluminum products. The current work studies the removal and behavior of  $\text{Al}_4\text{C}_3$  particles during flotation with different gas mixtures, as well as sedimentation. The interaction between carbide particles and  $\text{Al}_2\text{O}_3$  films during the melt treatment processes was also studied and reported. Factsage thermochemical software was used to model the interactions at the interface of inclusions and bubbles covered by films. The highest degree of carbide removal was obtained after flotation with an  $\text{H}_2\text{O}$ -containing argon gas mixture, where the carbide concentration dropped below the measured solubility limit of carbon at the corresponding temperature. Strong interaction between  $\text{Al}_4\text{C}_3$  particles and  $\text{Al}_2\text{O}_3$  films was observed during sedimentation which worked as an efficient removal method for the particles. Oxidation of carbides and formation of oxycarbides were suggested as the mechanisms promoting the attachment of carbides on oxide films.

<https://doi.org/10.1007/s11663-020-02049-7>  
© The Author(s) 2021

## I. INTRODUCTION

DURING aluminum production, different impurities contaminate the melt endo- or exogenously. Sedimentation and filtration are used as melt treatment methods aimed at removing solid particles such as borides, carbides, nitrides, and oxides. Gas purging/fluxing is used to remove dissolved elements such as hydrogen and alkali elements. Although gas purging and fluxing target the removal of dissolved elements, particles are to some extent also removed by flotation, which is a positive side effect of the gas purging process.<sup>[1]</sup>

Carbon, resulting in the formation of aluminum carbides in the melt, is introduced either during electrolysis, through contact with carbon anodes, or during melt processing, *via* reactions with different organic compounds. The solid solubility of carbon in aluminum is presumably very low and rarely—if ever—directly measured. The only available literature estimating the solid solubility of carbon in aluminum was authored by Obinata in the 1960s,<sup>[2]</sup> reporting 0.015 wt pct carbon solid solubility in aluminum—a concentration that is significantly higher than the later reported carbon solubilities in liquid Al by the literature discussed below. Carbon dissolved in the liquid largely precipitates as  $\text{Al}_4\text{C}_3$ <sup>[3]</sup> (Reaction 1) during cooling and solidification according to:

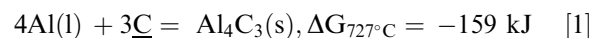


Figure 1 shows the aluminum carbide concentration due to the precipitation of dissolved carbon measured by Oden and McCune,<sup>[4]</sup> Rødseth *et al.*<sup>[5]</sup>, and Dorward<sup>[6]</sup> and Simensen<sup>[7]</sup> as a function of melt temperature. In,<sup>[4–6]</sup> aluminum was held in contact with pure graphite, ensuring carbon saturation in the melt. Oden and McCune<sup>[4]</sup> performed the measurements in the

MERTOL GÖKELMA is with the Department of Materials Science and Engineering, Norwegian University of Science and Technology, 7491, Trondheim, Norway and also with the Department of Materials Science and Engineering, Izmir Institute of Technology, 35430, Izmir, Turkey. Contact e-mail: mertolgokelma@iyte.edu.tr TRYGVE STORM AARNÆS, MARIA F. RENKEL, KAI ERIK EKSTRØM, and GABRIELLA TRANELL are with the Department of Materials Science and Engineering, Norwegian University of Science and Technology. JÜRGEN MAIER, and BERND FRIEDRICH are with the IME Process Metallurgy and Metal Recycling, RWTH Aachen University, 52056, Aachen, Germany.

Manuscript submitted May 11, 2020; accepted December 3, 2020.

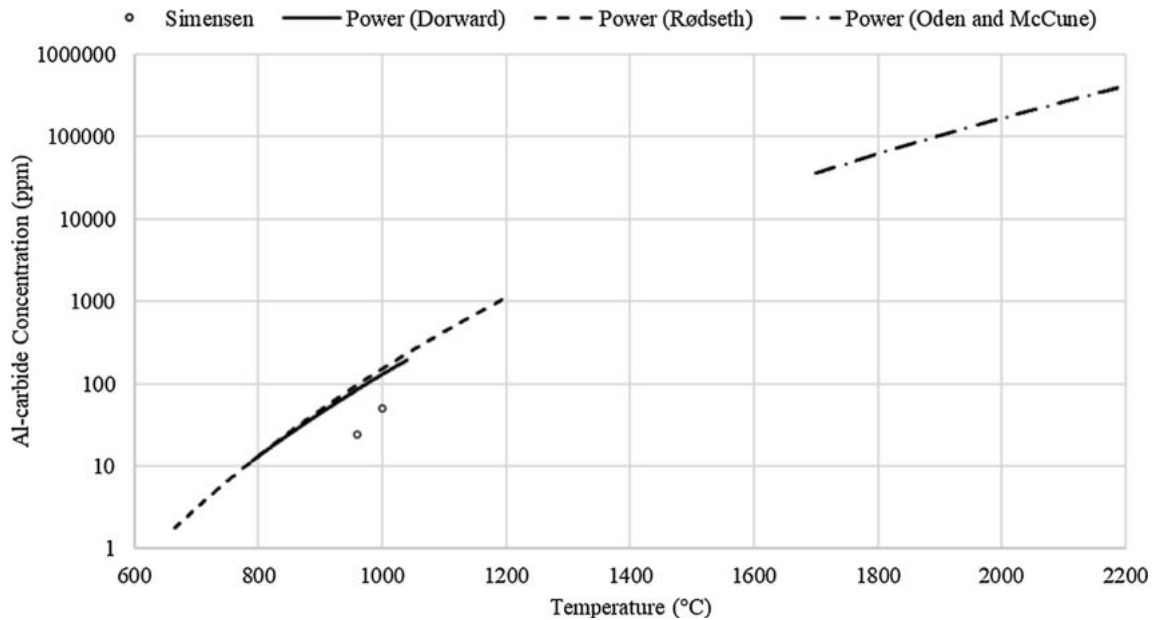


Fig. 1—The measured aluminum carbide concentration due to precipitation of dissolved carbon as a function of relevant melt temperature ranges<sup>[4-7]</sup>

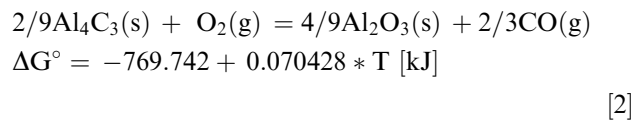
temperature range from 1700 °C to 2190 °C, Rødseth *et al.*<sup>[5]</sup> between 665 °C and 1200 °C, and Dorward<sup>[6]</sup> in the range from 790 °C to 1040 °C.

The results of Rødseth *et al.*<sup>[5]</sup> and Dorward<sup>[6]</sup> are in good agreement in the temperature range between 800 °C and 1050 °C. Simensen<sup>[7]</sup> performed ten measurements of samples from an operating electrolysis cell in temperature range of 960 °C to 1000 °C and the results showed a good agreement with Oden and McCune's results<sup>[4]</sup> after extrapolating the data to the relevant temperature range while Dorward<sup>[6]</sup> and Rødseth *et al.*<sup>[5]</sup> measured at least double the amount of aluminum carbides in the same temperature interval as Simensen.<sup>[7]</sup> Simensen noted that extrapolating such measurements over different temperatures may contain some uncertainties since carbon solubility in aluminum melts strongly depends on the temperature.<sup>[6]</sup>

The size of precipitated carbide particles is typically in the range of 0.1 to 5 μm in diameter<sup>[8]</sup> and may lead to surface defects and mechanical failures in thin wall aluminum products, due to the formation of Al(OH)<sub>3</sub> through reaction with moisture if not removed.<sup>[3]</sup> The small size of the particles makes their removal a challenge since filtration efficiency decreases sharply with decreasing inclusion size.<sup>[9,10]</sup> This may lead to an insufficient removal of the carbide inclusions if they have not formed larger clusters. In addition, the aluminum carbide density is very similar to that of liquid aluminum which leads to a very low inclusion sedimentation efficiency.

Dorward reported that any process, which promotes the adsorption of particles by foreign surfaces, will increase their removal.<sup>[3]</sup> Furthermore, the fine particle size and density of aluminum carbide particles may become advantageous in a flotation process rather than a settling process. Flotation with an inert gas may carry

the particles to the surface where they can be removed. Additionally, flotation with an oxygen containing gas may promote the attachment of particles on the bubbles *via* formation of an aluminum oxide layer on the bubble, leading to a better wetting between the particle and the bubble. The oxygen content in the gas might also lead to direct oxidation of carbides through reaction [2]:



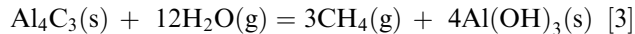
The removal efficiency of aluminum carbide particles must be improved in order to approach the quality requirements of inclusion-critical products. A better understanding of the behavior of carbides during melt treatment steps is crucial for improving the removal efficiency. This study hence focuses on the change in aluminum carbide concentration during inert and oxidative gas bubbling, or flotation, through the melt, as well as the interactions between oxides, gas bubbles, and carbides taking place during flotation and sedimentation processes.

## II. EXPERIMENTAL

### A. Materials

Primary aluminum, sampled from an electrolysis cell, was used in all experiments. The initial carbide concentration in the metal was measured to 35 ppm by the gas-chromatography method<sup>[8]</sup> at the Hydro Aluminum laboratories in Sunndalsøra, Norway. The metal samples were dissolved in a sodium hydroxide (NaOH) solution at a pressure of 10<sup>-5</sup> torr. The reaction gases were sampled (5 mL) with a syringe and analyzed in a

gas-chromatograph equipment. The amount of aluminum carbide was calculated by comparing the gas peak with that of a reference sample, having a known methane content. The decomposition of the aluminum carbide in the solution will take place through reaction [3]:



## B. Experimental Setup and Procedure

### 1. Experimental setup 1: study of $\text{Al}_4\text{C}_3$ concentration changes in gas-purged melts

For each experiment, 1 kg of the primary aluminum was placed in an alumina crucible, having a 1L capacity, which in turn was placed in a clay-bonded graphite crucible to avoid contact between the graphite and the melt. The assembly was placed in a 75 kW induction furnace and fitted with a hood for purging argon over the melt surface and for collecting off-gas for analysis. An alumina filter (60 ppi) connected to an alumina tube was immersed into the melt to introduce different gas mixtures. Argon (Ar), Ar- $\text{H}_2\text{O}$ , Ar- $\text{CO}_2$ , and Ar- $\text{O}_2$  gas mixtures were used to study the behavior and removal of carbides *via* different gas compositions. The gas blowing was applied for 30 minutes with a flow rate of 2 L/min after the melt reached the target temperature. The experimental layout and experimental parameters are presented in Figure 2 and Table I, respectively.

Samples for carbide analysis were taken with a syringe from the melt after blowing in experiment set 2 and by cutting a sample of the solidified melt after the experiment in set 1. The off-gas during the trials was analyzed by FTIR (Fourier-transform infrared spectroscopy) and Testo flue gas analyzer. CO and  $\text{CH}_4$  were measured by

the FTIR and CO,  $\text{CO}_2$ , and  $\text{O}_2$  with the Testo flue gas analyzer. No gas analysis was performed for trials 3 and 4 since the gas analysis was used for measuring the moisture content of the inlet gas.

The aluminum carbide content of the reacted metal and the resulting oxide taken after flotation trials was measured by gas-chromatographic analysis, see Section II-A.

### 2. Experimental setup 2: study of the behavior of inclusions during gas purging

Approximately 600 g of the primary aluminum was melted in a boron nitride-coated graphite crucible, having a 0.3 L capacity, in a resistance heated furnace. 25 g of aluminum foil was charged together with the primary aluminum pieces to generate oxide films and a graphite rod was held in the melt to ensure an excess of carbon. After the melt temperature reached melting point, argon (5.0) gas was introduced into the melt through a 60 ppi filter and the crucible was removed from the furnace straight after to let the melt solidify rapidly during gas purging. The trial was performed to entrap the bubbles during solidification and observe the inclusion removal mechanism rather than conducting a parametric study. The experimental setup and parameters are shown in Figure 3 and Table II, respectively. Samples of the solidified melt around the filter, as well as the dross, were mounted in epoxy and examined by scanning electron microscopy (SEM) to characterize inclusions/particles and films in the solidified material.

### 3. Experimental setup 3: study of the behavior of $\text{Al}_4\text{C}_3$ during sedimentation

Sedimentation trials were performed in a smaller laboratory scale resistant heating furnace. 50 g of primary aluminum, 13 g of an AlMg alloy (to generate more oxides), and 2 g of aluminum foil (to generate

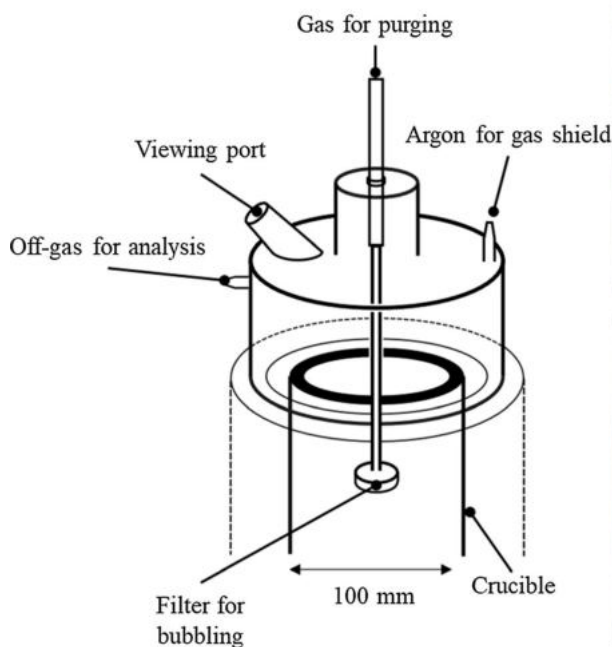
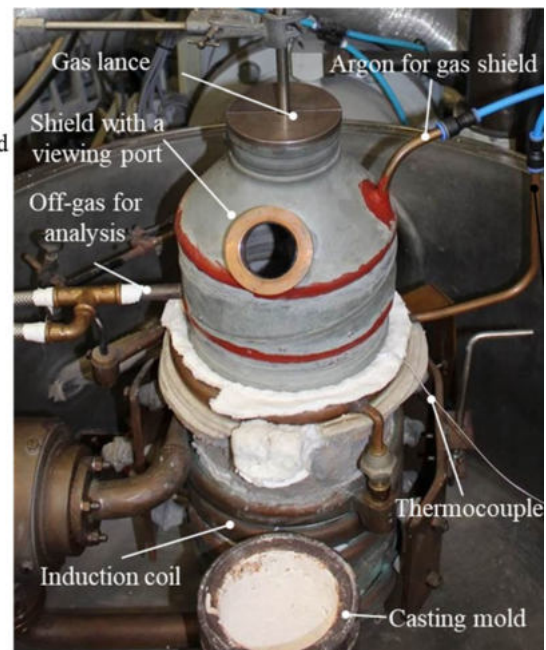


Fig. 2—Experimental setup of gas purging experiments.



**Table I. Experimental Parameters for the Gas Purging Experiments**

#		Gas Composition	Temperature (°C)	Sampling	Off-Gas Analysis
1	Set 1	Pure Ar	700	after solidication	CO, O <sub>2</sub>
2		Pure Ar	700		CO, O <sub>2</sub>
3		H <sub>2</sub> O 2 pct in Ar	700		—
4		H <sub>2</sub> O 2 pct in Ar	700		—
5		O <sub>2</sub> 10 pct in Ar	700		CO, O <sub>2</sub>
6		O <sub>2</sub> 10 pct in Ar	700		CO, O <sub>2</sub>
7		CO <sub>2</sub> 10 pct in Ar	700		CO, CO <sub>2</sub> , O <sub>2</sub>
8		CO <sub>2</sub> 10 pct in Ar	800		CO, CO <sub>2</sub> , O <sub>2</sub>
9	Set 2	Pure Ar	700	with a syringe from the melt	CO, CH <sub>4</sub>
10		Pure Ar	700		CO, CH <sub>4</sub>
11		Pure Ar	700		CO, CH <sub>4</sub>
12		H <sub>2</sub> O 1 pct in Ar	700		CO, CH <sub>4</sub>
13		H <sub>2</sub> O 1 pct in Ar	700		CO, CH <sub>4</sub>
14		H <sub>2</sub> O 2 pct in Ar	700		CO, CH <sub>4</sub>
15		H <sub>2</sub> O 2 pct in Ar	700		CO, CH <sub>4</sub>
16		H <sub>2</sub> O 2.5 pct in Ar	700		CO, CH <sub>4</sub>
17		H <sub>2</sub> O 2.5 pct in Ar	700		CO, CH <sub>4</sub>

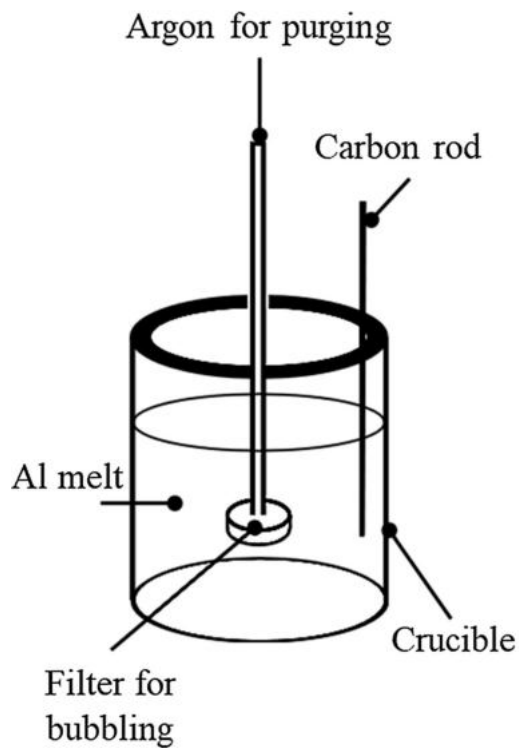


Fig. 3—Experimental setup for studying particle behavior during flotation.

**Table II. Experimental Parameters for the Carbide Behavior During Gas Purging**

Materials (gr)	Melt Temperature When Gas Purging Started (°C)	Solidification Time (min)	Gas Flow Rate (L/min)
600 Primary Al + 25 Al Foil	662	5	9

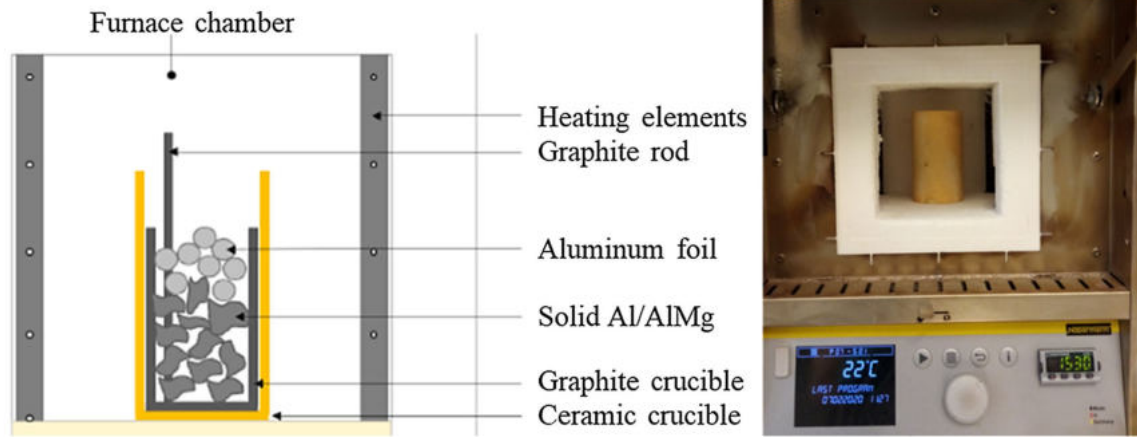


Fig. 4—Experimental setup for studying particle behavior during sedimentation.

alumina films) were melted in a graphite crucible. A graphite crucible was used to ensure enough aluminum carbides for the study. The experimental setup and parameters are shown in Figure 4 and Table III, respectively. When reaching 720 °C, the melt was held for 90 minutes for sedimentation. After being solidified, the cylindrical solid was cut into slices from top to bottom to observe the sedimentation behavior of inclusions.

### III. RESULTS

#### A. Change in $Al_4C_3$ Concentration During Gas Blowing

The first set of experiments tested the influence of different gas mixtures on the removal of aluminum carbide. In the first set of experiments, sampling was performed by cutting an edge of the solidified material representative for each trial and the results can be used to compare the effect of different gas mixtures. However, the results may be affected by an uneven distribution of particles through the melt during solidification. Hence, in the second set of experiments, sampling of the metal post-gas blowing was carried out using a syringe before solidification, as a comparison.

Figure 5 presents the aluminum carbide content in the melt and the dross after 30 minutes of purging with the different gas mixtures. Although the gas composition and the melt temperature affected the final  $Al_4C_3$  concentration in the melt, all results lie below the results reported in the literature. Purging using Ar and Ar- $O_2$  gas mixtures showed similar results with final carbide concentrations around  $1.5 \pm 0.3$  ppm in the melt and  $33 \pm 6$  ppm in the dross while Ar- $H_2O$  displayed lower concentrations in the melt, of  $1.1 \pm 0$  ppm carbide and  $70 \pm 45$  ppm in the dross. Flotation with Ar- $CO_2$  at 700 °C showed slightly higher carbide content (2.1 ppm) than all other gas mixtures and was repeated at 800 °C in order to study the possible effect of the Boudouard reaction (Eq. [4]) in removal of dissolved carbon in a C-saturated melt. This trial showed almost four times higher carbide content in the sample (7 ppm) and double the amount of CO in the off-gas, indicating that the

predominant reaction is a carbide-forming reaction with aluminum oxide and CO as reaction products (Eq. [5]). The aluminum carbide concentrations detected in the dross were 1000 and  $3000 \pm 0$  ppm at 700 °C and 800 °C, respectively.

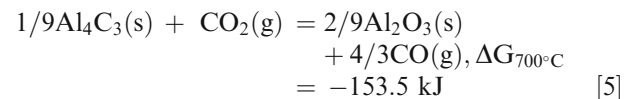


Figure 6 shows the CO,  $CO_2$ , and  $O_2$  concentration in the off-gas during the first set of purging trials. No off-gas data were measured during the trial with Ar- $H_2O$  due to measurement of the moisture content in the inlet gas instead. A sudden peak of CO was observed in all experiments in the first seconds after gas purging started. During purging with Ar, the CO peak appeared twice during flotation and the decrease in concentration was not as fast as it was during flotation with Ar- $O_2$ . The CO concentration in the off-gas during purging with the Ar- $CO_2$  mixture was significantly higher than that using Ar and Ar- $O_2$ , and it remained constant at approximately 300 ppm at 700 °C and 650 ppm at 800 °C due to the continuous conversion of  $CO_2$  to CO.

In the second set of experiments,  $O_2$  and  $CO_2$ -containing gases were not utilized due to high dross and carbide formation, respectively. Additional trials were performed with Ar and Ar- $H_2O$  to study their effects on the removal of carbides in more detail. All samples were taken by a syringe after flotation to ensure that the carbide concentration was representative for the entire melt.

Figure 7 presents the  $Al_4C_3$  concentration of the samples taken after 30 minutes of gas purging. Purging with Ar achieved reduction of the carbide concentration down to 2.2 ppm (in av.  $4.3 \pm 2.1$ ) while purging with Ar- $H_2O$  reduce it down to 1.8 ppm (in av.  $2.6 \pm 0.9$ ) at 700 °C. The trials with different  $H_2O$  content in the gas (1, 2, or 2.5 pct) did not show a significant difference

**Table III. Experimental Parameters for the Carbide Behavior During Sedimentation**

Materials	Melt Temperature (°C)	Holding Time (min)
50 gr Primary Al + 13 gr AlMg + 2 gr Al Foil	720	90

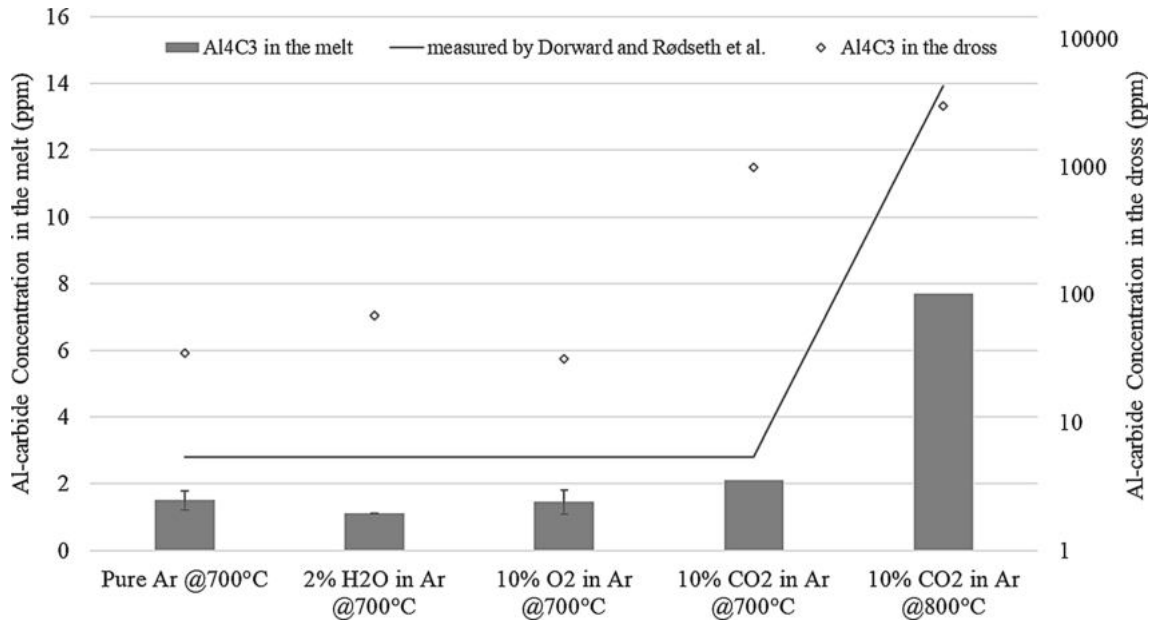


Fig. 5—Concentration of aluminum carbide in the melt and dross (in log scale) after flotation for 30 min with different gas mixtures (Set1, sampled from solid material).

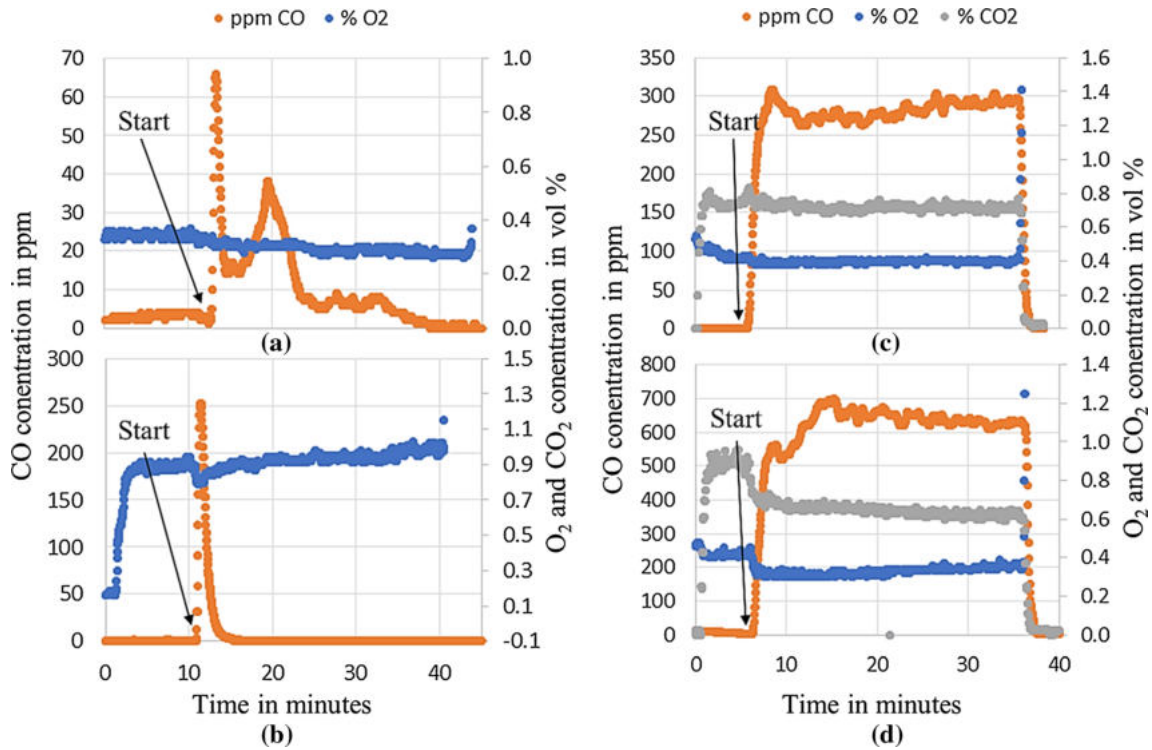


Fig. 6—Off-gas concentration of CO, O<sub>2</sub>, and CO<sub>2</sub> during flotation with (a) Argon at 700 °C, (b) Argon-10 pct O<sub>2</sub> at 700 °C, (c) Argon-10 pct CO<sub>2</sub> at 700 °C, (d) Argon-10 pct CO<sub>2</sub> at 800 °C, measured by TESTO flue gas analyzer.

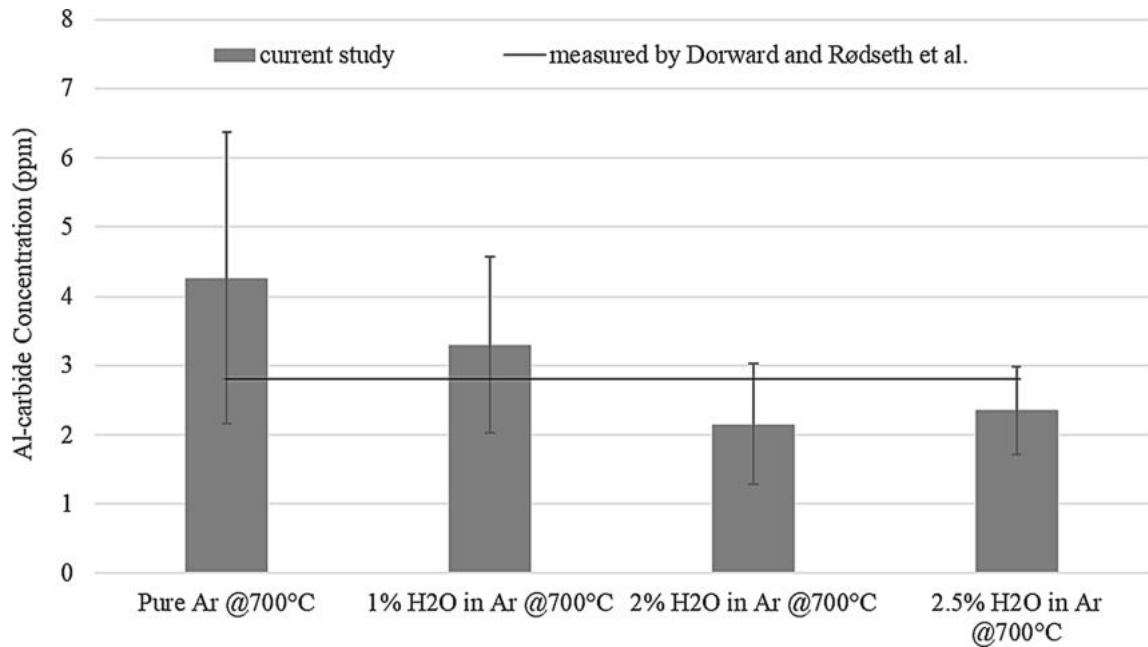


Fig. 7—Concentration of aluminum carbide after flotation for 30 min with pure argon and 1, 2, and 2.5 pct H<sub>2</sub>O in argon (Set2).

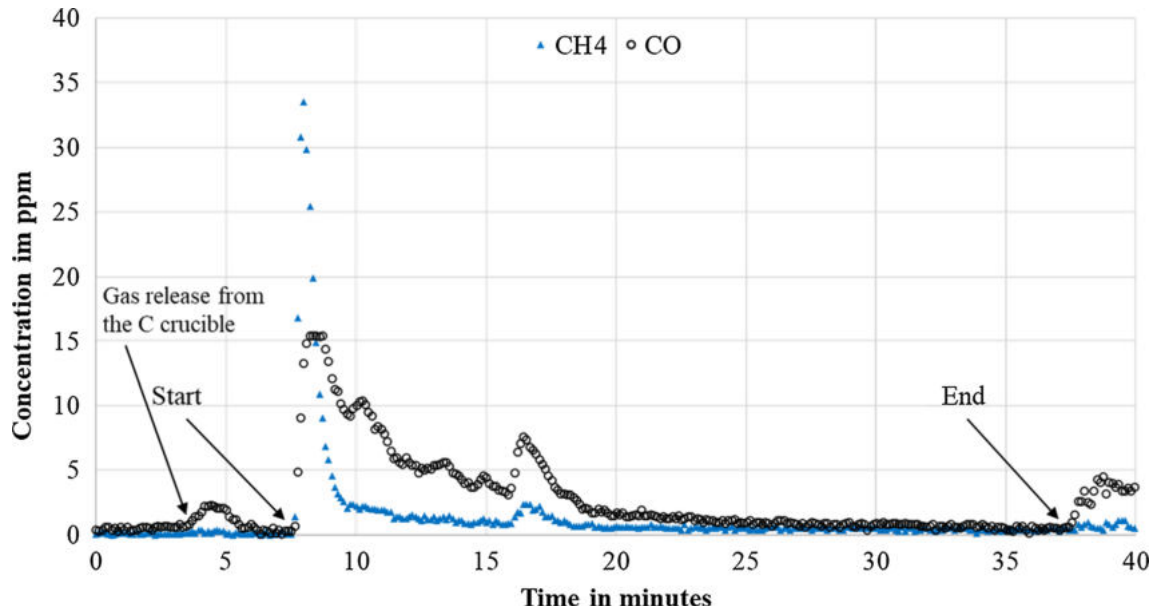


Fig. 8—CO and CH<sub>4</sub> formation during flotation with Argon-H<sub>2</sub>O mix measured by FTIR.

between trials; however, most of the measured data lie below the measured saturation concentrations by Rødseth *et al.*<sup>[5]</sup> and Dorward<sup>[6]</sup>

Figures 8 and 9 show the CO and CH<sub>4</sub> concentration measured in the off-gas during purging. A sudden increase in both gas concentrations was observed right after starting the bubbling, similarly to what was previously observed in the measurements of the first set.

### B. Behavior of Inclusions During Flotation

Samples with trapped gas bubbles, achieved by rapid solidification of the samples generated using the experimental setup 2, were cut and analyzed in the SEM. Figure 10 presents the particles captured by such bubbles. The bubble size was measured between 0.2 and 0.5 mm and inclusions on the bubbles were in the range of 20–50 μm. It is likely that these particles are aluminum oxide particles since they are larger than

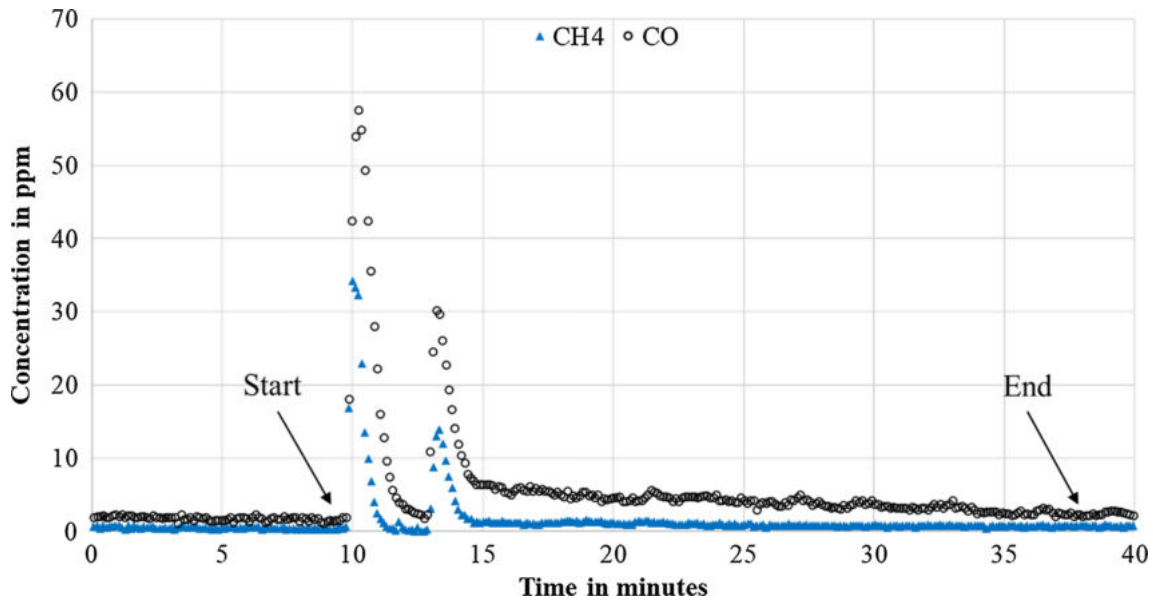


Fig. 9—CO and CH<sub>4</sub> formation during flotation with Argon measured by FTIR.

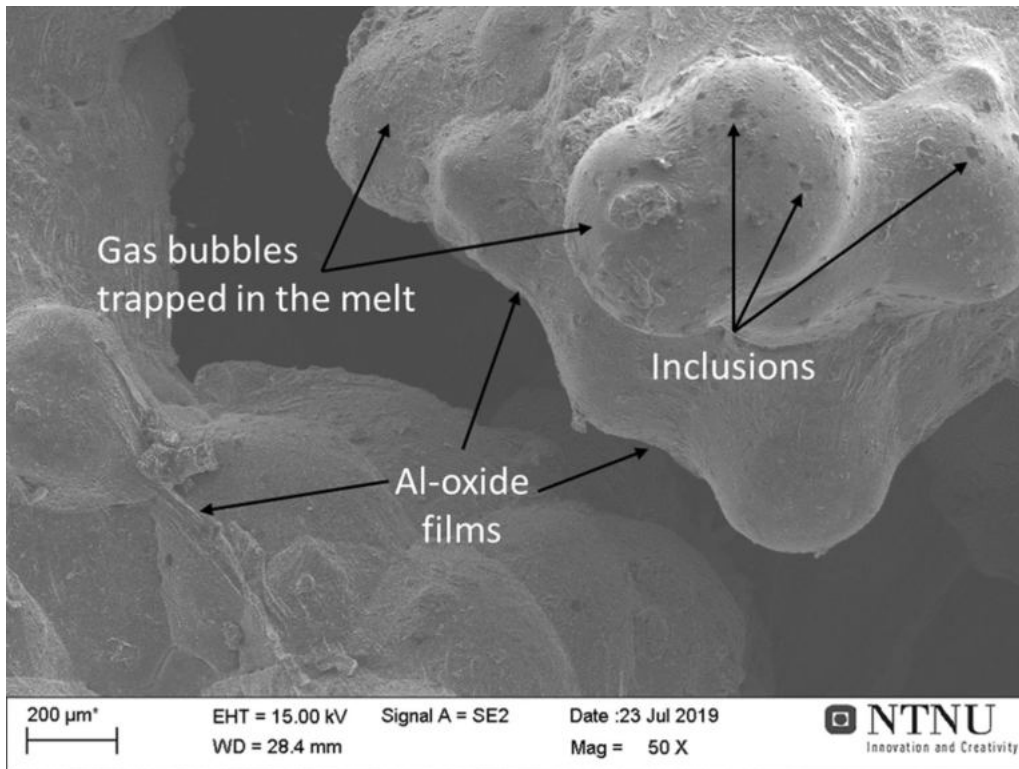


Fig. 10—Inclusions attached to bubbles during flotation in an aluminum melt.

typical aluminum carbide particles. Higher magnification and EDS analysis were not possible to perform since the samples could not be polished sufficiently due to very porous and uneven structure.

After solidification, dross samples were prepared and analyzed by SEM. Figure 11 shows a SEM image of the dross after flotation. Inclusions found in the samples were in the typical size range of aluminum carbide



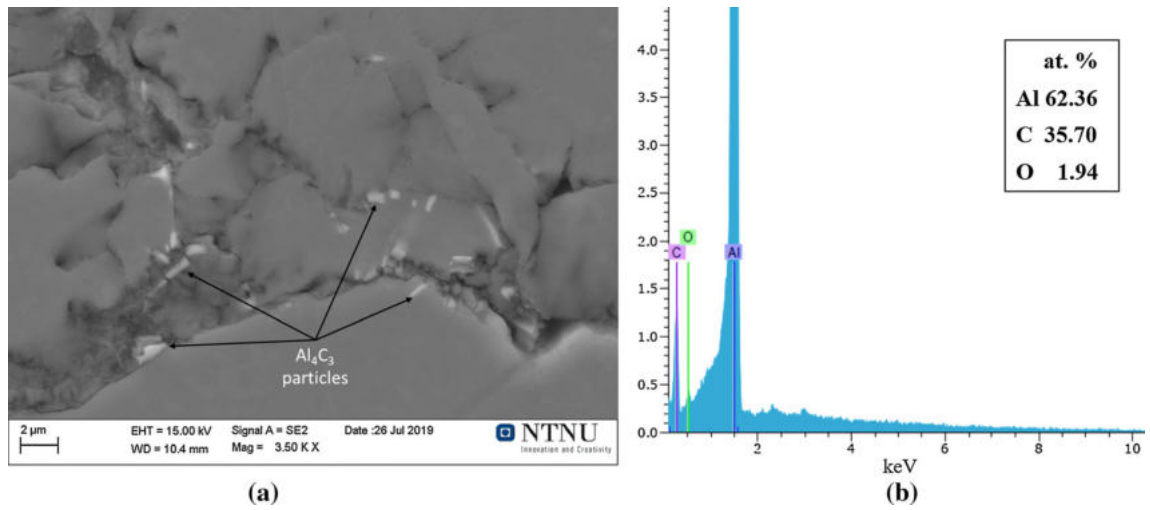


Fig. 11—(a)  $Al_4C_3$  particles entrapped by the dross during flotation, (b) EDS graph of detected particles in the dross.

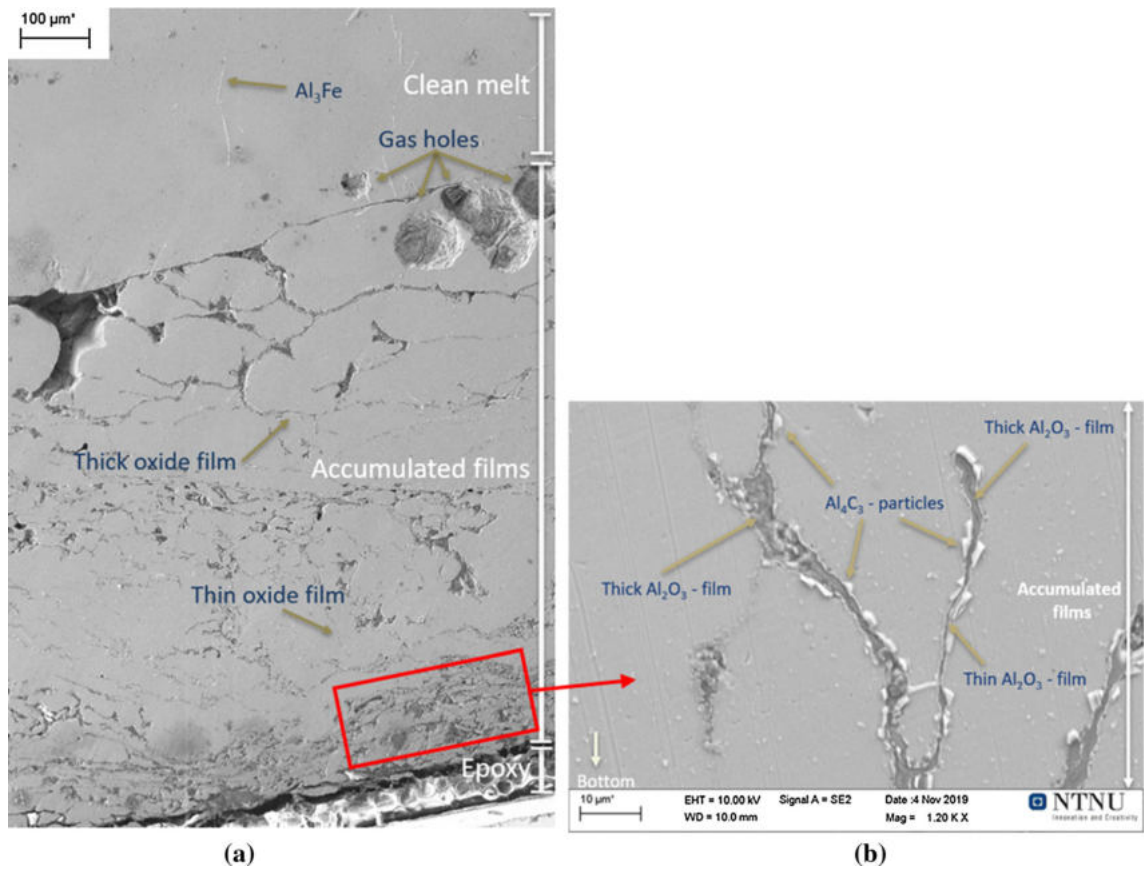


Fig. 12—(a) SEM image of inclusions settled to the bottom of the melt, (b) settled  $Al_4C_3$  particles captured by the surface of the oxide films.

particles and Al-C peaks were detected by the EDS analysis, indicating that the particles are aluminum carbide inclusions removed from the melt by floating bubbles.

### C. Behavior of $Al_4C_3$ During Sedimentation

Cross sections of the samples after the sedimentation experiments were prepared and studied in the SEM to investigate particle/film accumulation due to settling. The total height of the solid sample was 50 mm and the

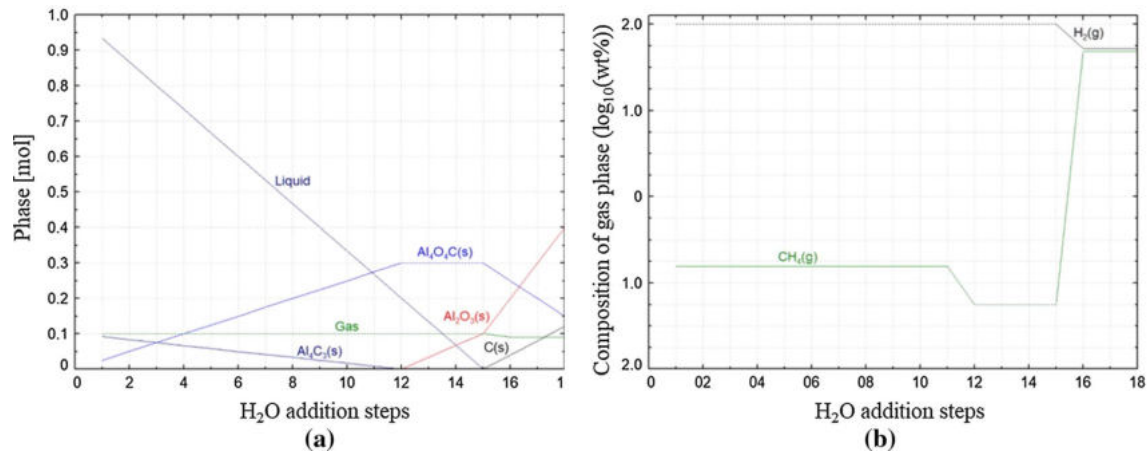


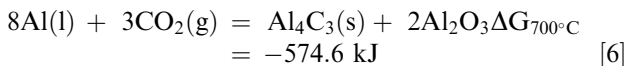
Fig. 13—Thermodynamic calculations of a C-saturated aluminum smelt, with the addition of H<sub>2</sub>O on the x-axis at 700 °C. *FactSage 7.3* (a) composition of solid phases, (b) composition of gaseous phases.

sediment was found in the bottom part of the crucible as a 700 μm thick area that corresponded to 1.4 pct of the total melt height. This part of the material contained a high number of thin and thick alumina films, as well as carbide particles. In the upper part of the sample, virtually no inclusions were found.

Figure 12(a) shows a picture from the region where the inclusions settled during sedimentation. This area contains settled alumina films with numerous captured particles. Multiple Al-O peaks and Al-C peaks were detected by the EDS analysis of films and particles, respectively. Al<sub>4</sub>C<sub>3</sub> particles with a size below 5 μm were found attached on the both sides of thin and thick Al<sub>2</sub>O<sub>3</sub> films (Figure 12(b)).

#### IV. DISCUSSION

Purging of carbide-containing aluminum melts with different gas mixtures results in different final carbide concentrations. Besides the particle flotation effect of the gas, it was observed that the Ar-CO<sub>2</sub> mix generates new carbides and thus significantly increases the concentration of Al<sub>4</sub>C<sub>3</sub> particles in the dross by CO<sub>2</sub>-induced oxidation of the Al metal, according to reaction [5]. A variation of Eq. [6] is the simultaneous generation of Al<sub>4</sub>C<sub>3</sub>, Al<sub>2</sub>O<sub>3</sub>, and CO through reaction between Al and CO<sub>2</sub>. An accumulation of carbides up to 3000 ppm was measured in the dross after flotation with Ar-CO<sub>2</sub>, while a maximum of 100 ppm was observed for the other gas mixtures.

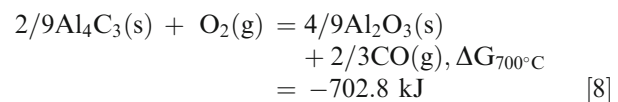
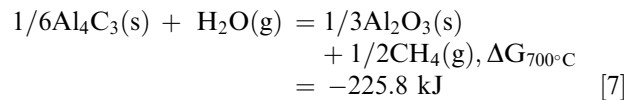


CO and CH<sub>4</sub> peaks were observed in the early stages of gas purging for all trials, and the sudden peaks appearing in the start of the trials can be attributed to the direct oxidation of carbides. This oxidation might originate from two mechanisms:

1. The Al<sub>4</sub>C<sub>3</sub> particles are oxidized in the melt by the flotation gas (reactive) mixtures

2. Al<sub>4</sub>C<sub>3</sub> particles, attached to crucible walls or underneath the oxide layer due to poor wetting, are carried to the melt surface by the gas (reactive or noble) and oxidized by the air above the melt surface/the purge gas mixture. The additional effect of gas bubbles breaking the oxide film, with subsequent exposure/detachment of carbides, enhances the oxidation effect.

The overall oxidation of particles may theoretically occur through reactions (6 through 8) with a subsequent formation of CO and/or CH<sub>4</sub> depending on the composition of the purging gas. Purging with only Ar may have the oxidation effect through reaction [8] due to very low oxygen content in the gas. The oxidation will occur through reactions [5], [8], and [7] through [8] while purging with Ar-CO<sub>2</sub> and Ar-H<sub>2</sub>O, respectively.



Most of the trials show a lower final concentration of aluminum carbides after purging with Ar-H<sub>2</sub>O gas compared to other gas mixture. The clear CH<sub>4</sub> release must be due to the carbide oxidation *via* H<sub>2</sub>O since here is no other C source in the system.

##### A. Carbide Oxidation by H<sub>2</sub>O

Thermodynamic calculations were performed to study the mechanism behind the oxidation of carbide particles *via* H<sub>2</sub>O, using FactSage 7.3 thermochemical software.<sup>[1]</sup> Descriptions of oxide solutions were taken from the FToxide database, liquid aluminum (liquid) from the FTlite database, and carbides and oxycarbides from the FTOxCN database. Thermodynamic properties of pure gas and solid species were taken from the

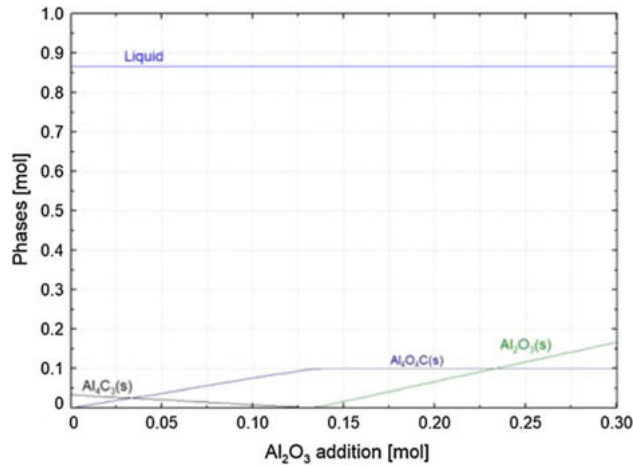
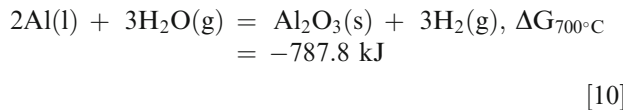
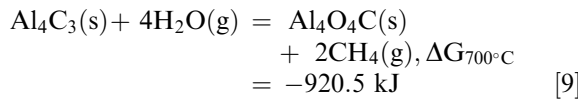
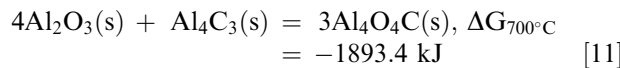


Fig. 14—Thermodynamic calculations where  $\text{Al}_2\text{O}_3$ , on the x-axis, is added to a C-saturated aluminum melt at 700 °C. *FactSage 7.3*.

FactPS database. Gaseous  $\text{H}_2\text{O}$  was added to a C-saturated pure liquid aluminum at 700 °C, as shown in Figure 13. The open calculations predict that  $\text{Al}_4\text{C}_3(\text{s})$  oxidizes in reaction with  $\text{H}_2\text{O}(\text{g})$  in the bubble and form  $\text{Al}_4\text{O}_4\text{C}(\text{s})$  simultaneously with  $\text{Al}(\text{l})$  oxidation, forming  $\text{Al}_2\text{O}_3$  while  $\text{H}_2(\text{g})$  and  $\text{CH}_4(\text{g})$  are released (reactions 7, 9, 10):



A subsequent reaction between oxide formed on the bubble surface and carbides in the melt, forming oxycarbide, as expressed by reaction [11] may take place (Figure 14). The Gibbs energy of formation of  $\text{Al}_4\text{C}_3$  is  $-159 \text{ kJ}$  at 727 °C<sup>[12,13]</sup> while it is  $-1893.4 \text{ kJ}$  for  $\text{Al}_4\text{O}_4\text{C}$  at 700 °C. This comparison of the Gibbs free energy values shows that the oxycarbide formation is thermodynamically feasible; however, it is kinetically less likely since both phases are in solid form.



The carbide oxidation on the melt surface does not occur to the same extent in all cases due to the formation of a surface oxide layer. This was observed by either a sudden or gradual decrease in  $\text{CH}_4$  and  $\text{CO}$  peaks during gas purging, depending on the formation of an oxide layer on top of the melt. A thick oxide layer might act as an isolative layer during the initial stages of purging, which can capture particles and hinder further oxidation as opposed to a thin oxide layer with disturbance or splashing, which may let particles oxidize immediately when reaching the melt surface.

## B. Measured Carbide Concentration in Al for $\text{H}_2\text{O}$ -Containing Gas Purging

The removal *via* oxidation, discussed above, does not explain the reason why the measured final carbide concentration after gas purging with  $\text{H}_2\text{O}$ -containing gases is below the values corresponding to the carbon solubility limit measured by Rødseth *et al.*<sup>[5]</sup> and Dorward.<sup>[6]</sup> If we accept these data as correct, two mechanism may explain a lower  $\text{Al}_4\text{C}_3$  content than that expected:

1. Precipitation of dissolved C through local cooling on the bubble surface:

The bubbles enter the melt at room temperature and promote local carbide precipitation on the colder surface rather than in the melt, due to the local change in C solubility. Local cooling might help to remove dissolved carbon as carbide and formation of hydroxides and oxycarbides might promote attachment of particles to the bubble surface which will lead to better removal rates. Precipitated carbides due to local cooling may dissolve back as Al and C, but this dissolution is controlled by the kinetics mainly affected by the surface area of the carbide particle and retention time in the melt during flotation and may hence not occur during the short residence time of the bubble-attached precipitate.<sup>[14]</sup> On the other hand, the exothermic formation of alumina on the bubble surface may decrease the duration needed for the bubble to reach the equilibrium temperature.

2. Removal of the excess C precipitated as  $\text{Al}_4\text{C}_3$  by magnetic stirring and floating bubbles:

The removal rates reported from the current work, as opposed to the values determined by Rødseth *et al.*<sup>[5]</sup> and Dorward,<sup>[6]</sup> may be due to the removal of entrapped carbides, on crucible walls or underneath the oxide layer, with the stirring effect of the gas purging rather than performing measurements in a melt without any disturbance. The remaining carbides in the melt at any temperature may affect the measured  $\text{Al}_4\text{C}_3$  concentration which is the sum of the suspended carbides in the melt ( $C_{\text{Al}_4\text{C}_3}$ ) and the carbides precipitated due to dissolved carbon ( $C_{\text{C}}$ )<sup>[7]</sup>:

$$C = C_{\text{Al}_4\text{C}_3} + 4 \cdot C_{\text{C}} \quad [12]$$

## C. Alternative Data on the Solubility of Carbon in Aluminum (in Contrast with the Data Reported by Rødseth *et al.*<sup>[5]</sup> and Dorward<sup>[6]</sup>)

Oden and McCune<sup>[4]</sup> measured the aluminum carbide concentration due to precipitation of dissolved carbon which is in agreement with the data reported by Simensen.<sup>[7]</sup> The solubility of carbon (by weight) was as follows:

$$C_{\text{C}} = 1511 \cdot \exp(-23797/T) \quad [13]$$

The measurements were performed at high temperature as mentioned in Figure 1 but the solubility data at low temperatures can be obtained by extending the trend down to 700 °C. According to the extended data,

the carbon solubility is approximately 0.15 ppm which corresponds to  $\approx 0.6$  ppm of aluminum carbide at 700 °C. If these data are considered as correct, it means we still have unremoved aluminum carbide particles in addition to dissolved carbon.

#### D. Benefits of Gas Purging for Carbide Removal

Aluminum carbide particles can be easily removed by flotation since they are small and have a similar density to the aluminum melt. The density of aluminum carbide particles is 2360 kg/m<sup>3</sup> and the density of a pure aluminum melt varies between 2391 kg/m<sup>3</sup> and 2356 kg/m<sup>3</sup> at typical melt treatment temperatures between 660 °C and 775 °C, respectively. The settling velocities according to Stokes drag law lay between  $-0.00004$  and  $0.0003$  mm/s for particles with the diameter of 5  $\mu$ m. It was reported by Sztur *et al.*<sup>[15]</sup> that the maximum melt velocity is up to 3 mm/s in laboratory furnaces and up to 15 mm/s in industrial furnaces due to natural convection. These values are considerably higher than the relative velocities of aluminum carbide particles which will be easily dragged by the melt and hinder the sedimentation process.

The settling behavior of carbides agglomerated on alumina films is, however, different from that of single particles. Attached carbides on films might act as a carbon source in the melt which hinders the reduction in carbide concentration during remelting by back dissolving as carbon. This rises the importance of flotation with a special focus on inclusion removal (agglomerated films and carbides) as well as final melt temperature before casting as mentioned in the previous study on the remelting effect on the carbide concentration.<sup>[16]</sup> With this method, carbide particles can be entrapped by the dross and skimmed off. Even if the dross does not capture the particles, carbides may oxidize on the surface which will avoid them behaving as a carbon source due to a stable aluminum oxide shell around the particle.

## V. CONCLUSIONS

Behavior of aluminum carbide particles during flotation with different gas mixtures and interaction with oxide films during sedimentation was studied. The following conclusions can be drawn from the results:

- Oxidation of aluminum carbides with O<sub>2</sub> or H<sub>2</sub>O-containing gases occurs on the bubble and/or melt surface during gas purging/flotation with a subsequent formation of CO and CH<sub>4</sub>
- H<sub>2</sub>O-containing bubbles lead to Al<sub>2</sub>O<sub>3</sub> formation on the bubble. Oxide and/or oxycarbide formation in the interface might promote attachment of particles on the bubbles and increase the removal efficiency.
- A strong clustering tendency between aluminum carbide particles and oxide films was observed. The attachment of particles on films promoted the removal of carbides *via* sedimentation on the oxide film. The carbide particles settled with films do not repre-

sent the dissolved carbon concentration which will precipitate during solidification.

## ACKNOWLEDGMENTS

The authors wish to thank staff at Hydro Aluminium Sunndalsøra for supplying electrolysis metal and for carrying out all carbide analyses. The work was funded through the “BEST” project, jointly financed by the Research Council of Norway, Hydro Aluminium, Alcoa Norway, Granges Aluminium and Hycast.

## OPEN ACCESS

This article is licensed under a Creative Commons Attribution 4.0 International License, which permits use, sharing, adaptation, distribution and reproduction in any medium or format, as long as you give appropriate credit to the original author(s) and the source, provide a link to the Creative Commons licence, and indicate if changes were made. The images or other third party material in this article are included in the article's Creative Commons licence, unless indicated otherwise in a credit line to the material. If material is not included in the article's Creative Commons licence and your intended use is not permitted by statutory regulation or exceeds the permitted use, you will need to obtain permission directly from the copyright holder. To view a copy of this licence, visit <http://creativecommons.org/licenses/by/4.0/>.

## REFERENCES

1. G. Gaustad, E. Olivetti, and R. Kirchain: *Resour. Convers. Recycl.*, 2012, vol. 58, pp. 79–87.
2. I. Obinata and N. Komatsu: *J. Jpn. Inst. Light Met.*, 1964, vol. 14 (4), pp. 226–30.
3. R. Dorward: *Aluminum*, 1973, vol. 49 (10), pp. 686–89.
4. L.L. Oden and R.A. McCune: *Met. Trans. A*, 1987, vol. 18A, pp. 2005–14.
5. J. Rødseth, B. Rasch, O. Lund, J. Thonstad, *Light Met.*, 2002, pp. 883–88.
6. R. Dorward: *Metal Trans. A*, 1990, vol. 21A, pp. 255–57.
7. C.J. Simensen: *Met. Trans. A*, 1989, vol. 20A, p. 191.
8. C.J. Simensen: *Zeitschrift Für Analytische Chemie*, 1978, vol. 292 (3), pp. 207–12.
9. N.J. Keegan, W. Schneider, and H.P. Krug, *Light Met.*, 1999, pp. 1031–41.
10. L.N.W. Damoah and L. Zhang: *Metall. Mater. Trans. B*, 2010, vol. 41B, pp. 886–907.
11. C.W. Bale *et al.* *Calphad*, vol. 54, pp. 35–53.
12. C. Qiu and R. Metselaar: *J. Alloys Compd.*, 1994, vol. 216 (1), pp. 55–60.
13. U.V. Choudary and G.R. Belton: *Metall. Trans. B*, 1977, vol. 8 (4), pp. 531–34.
14. T. Rosenqvist: *Principles of Extractive Metallurgy*, 2nd ed., Tapir Academic Press, Trondheim, 2004.
15. C. Sztur, F. Balestreri, J. Meyer, B. Hannart, *TMS Light Met.*, 1990, pp. 107–14.
16. M. Göknelma, T.S. Aarnæs, J. Maier, B. Friedrich, G. Tranell, *TMS Light Met.*, 2020, pp. 1033–39.

**Publisher's Note** Springer Nature remains neutral with regard to jurisdictional claims in published maps and institutional affiliations.